Forum Original Research Communication

Tumor Suppressive Effects of MnSOD Overexpression May Involve Imbalance in Peroxide Generation Versus Peroxide Removal

LISA A. RIDNOUR,[1,3] TERRY D. OBERLEY,[2] and LARRY W. OBERLEY[3]

ABSTRACT

Manganese superoxide dismutase (MnSOD) activity is generally lower in cancer cells when compared with their normal cell counterparts. Many studies have shown that replacing the diminished MnSOD activity leads to inhibition of the malignant phenotype. We sought to overexpress MnSOD in a chemically transformed, malignant rat cell line with low endogenous MnSOD activity to determine the effect on the malignant phenotype. After *MnSOD* cDNA transfection, clonal populations were characterized at the molecular level for protein, RNA, and DNA, as well as for *in vitro* and *in vivo* growth and *in vivo* lung metastasis. *MnSOD* transfectants, which both under- and overexpressed MnSOD protein, were identified. These transfectants demonstrated variations in glutathione peroxidase and catalase activity levels, indicating differences in peroxide-generating versus peroxide-metabolizing enzymes (antioxidant imbalance); these differences were suggestive of alterations in their abilities to metabolize peroxide when compared with the parental cell line. In addition, these transfectants demonstrated reductions in both *in vitro* and *in vivo* growth, as well as a reduction in metastatic potential, which correlated with antioxidant imbalance. These results suggest that the tumor suppressive effect of MnSOD overexpression is in part mediated by an antioxidant imbalance resulting in the reduced capacity to metabolize increased levels of intracellular peroxides. *Antioxid. Redox Signal.* 6, 501–512.

INTRODUCTION

MANGANESE SUPEROXIDE DISMUTASE (MnSOD) is a mitochondrial antioxidant enzyme that catalyzes the dismutation of superoxide radical ($O_2^{\bullet-}$) to hydrogen peroxide (H_2O_2) and oxygen. MnSOD activity is in general diminished in cancer cells when compared with the normal cells from which they were derived (26, 29). Significant decreases in MnSOD activity compromise the cellular antioxidant defense system, which results in the accumulation of reactive oxygen species (ROS). At the molecular level, increased ROS lead to oxidant injury that is manifested as alterations in protein structure, membrane lipid peroxidation, DNA damage, and chromosomal aberrations, and are associated with a host of diseases, including cancer (7, 9, 24, 41).

If MnSOD is important in cancer, then normalization of the levels of MnSOD should result in reversal of at least part of the cancer cell phenotype. This hypothesis was first suggested by Oberley and Buettner in 1979 (26, 27) and has been tested in a number of ways with results in general confirming the hypothesis. The most important technique utilized to examine this hypothesis has been cDNA transfection. The first study using the cDNA transfection technique with MnSOD was published in 1993 (5). Church *et al.* demonstrated that the transfection of *MnSOD* cDNA into cultured human melanoma cells resulted in the loss of the malignant phenotype, both *in vitro* by assays such as growth in soft agar and *in vivo* by growth in nude mice. Similar results have been found in mouse fibrosarcoma (12, 38), MCF-7 human breast carcinoma (14), virally transformed WI-38 human lung fibroblasts

---

[1]Present address: Radiation Oncology Branch, National Cancer Institute, Bethesda, MD.
[2]Pathology and Laboratory Medicine Service, William S. Middleton Memorial Veterans Hospital, Madison, WI.
[3]Free Radical and Radiation Biology Program, Department of Radiation Oncology, University of Iowa, Iowa City, IA.

(48), A172R rat glioma (49), U118 human glioma (50), SCC-25 human oral squamous carcinoma (19), and DU 145 human prostatic carcinoma (15). In most cases, the maximal increases in MnSOD in these transfection studies were approximately sixfold, which approached the activity levels of their normal cell counterparts (~10-fold increase). Thus, the evidence appears substantial that stable MnSOD elevation by plasmid transfection can suppress the malignant phenotype in a variety of tumors. On the basis of this work showing growth suppression and the fact that loss of heterozygosity for *MnSOD* has been found in human melanoma (23) and glioma (18, 35), it has been proposed that *MnSOD* is a new type of tumor suppressor gene (4).

The purpose of this study was to evaluate the anticancer effects of MnSOD overexpression on the *in vitro* and *in vivo* properties of a chemically transformed, malignant rat fibroblast XR23M cell line (36), and to investigate further the involvement of antioxidant imbalance in the tumor suppressive effects of MnSOD. In this study, antioxidant imbalance is characterized by the ratio of peroxide-generating enzymes [superoxide dismutase (SOD)] to peroxide-metabolizing enzymes [glutathione peroxidase (GPx) and/or catalase (CAT)]. The results of this work demonstrate that antioxidant imbalance is indeed associated with the tumor suppressive effects of MnSOD in the XR23M malignant cell line. These results support the hypothesis of a role of antioxidant imbalance and ROS in cancer (16).

MATERIALS AND METHODS

Cell culture

XR23M is a chemically transformed rat cell line that was cloned from the nontumorigenic parental cell line X-REF-23 (XR23, *x*-ray immortalized rat embryo fibroblasts) following exposure to methylcholanthrene (44). The cells were routinely cultured in Dulbecco's modified eagle medium supplemented with 10% heat-inactivated fetal bovine serum and maintained at 37°C in an atmosphere of 95% room air and 5% CO_2. For experimental purposes, the cells were grown in 100-mm tissue culture dishes (Corning) seeded at a density of 10^5 cells per plate. The medium was changed every third day and 24 h prior to harvesting. Confluent cells were scrape-harvested in ice-cold phosphate-buffered saline, pH 7.0, and centrifuged. Cell pellets were stored at -20°C prior to further experimentation.

Transfection of expression plasmid

The pMET · MEX (pMM) plasmid, kindly provided by Dr. Yi Sun, contained an 0.8-kb mouse *MnSOD* cDNA insert cloned into the *Eco*RI site, which was driven by the metallothionein promoter (43). In this work, the cells were grown without zinc supplementation. The serum contained 2.5 μg/ml zinc, which may have allowed for maximal expression of the *MnSOD* cDNA insert. Moreover, although the metallothionein promoter is known to be inducible by zinc, studies have shown that it functions in the absence of inducing agents (1, 21). XR23M cells were transfected with Lipofectin reagent (GibcoBRL), and then neomycin-resistant

colonies were ring-isolated and maintained in culture for at least 6 weeks prior to characterization. The cells were plated for experimentation in complete media without neomycin.

Sample homogenate preparation

The frozen pellets were thawed slowly, resuspended in a 1:1 volume of 50 m*M* potassium phosphate buffer, pH 7.8, and then sonicated while on ice. Protein concentrations were determined by the method of Lowry *et al.* (20).

Western blotting

Western analysis was performed as described by Oberley *et al.* (28). The MnSOD, copper- and zinc-containing SOD (CuZnSOD), CAT, and GPx antibodies used in this work were developed in our laboratory (30–32). Protein samples were loaded on 12.5% (MnSOD and CAT) or 15% (CuZnSOD and GPx) polyacrylamide gels and electrophoresed at 100 V for 2 h. The protein was transferred onto nitrocellulose paper (Schleicher & Schuell) as described (45). The blots were blocked for 2 h at room temperature and then incubated at 4°C in diluted antibody overnight. Immunoreactive protein was visualized by alkaline phosphatase and BCIP (5-bromo-4-chloro-3-indolyl phosphate) colorimetric staining.

SOD activity assay

SOD activity was measured by the method of Spitz and Oberley (40). This assay is based upon the reduction of nitro blue tetrazolium (NBT) to blue formazan by $O_2^{\cdot-}$. One unit of SOD activity was defined as the amount required to yield 50% of sample maximum inhibition of NBT reduction by $O_2^{\cdot-}$. MnSOD was discerned from CuZnSOD by the addition of 5 m*M* sodium cyanide.

Southern blot analysis

DNA was isolated according to standard procedures. Fifteen-microgram aliquots of *Eco*RI-digested DNA were loaded on an 0.8% agarose gel (Kodak) containing 0.5 μg/ml ethidium bromide (Sigma Chemical Co., St. Louis, MO, U.S.A.) and electrophoresed overnight at 20 V. The DNA was transferred overnight onto a positively charged nylon membrane (Boehringer Mannheim) and then baked at 80°C for 1 h. The blotted DNA was probed with freshly boiled digoxigenin-(Boehringer Mannheim) labeled *MnSOD* cDNA in a 42°C circulating water bath overnight (39). The hybridized membrane was then washed several times, and bound probe was detected using chemiluminescence from Lumigen PPD [4-methoxy-4-(3-phosphatephenyl)spiro(1,2-dioxetane-3,2′-adamantane)].

Detection of MnSOD gene expression

Total RNA was isolated from confluent cell monolayers as described (34). Expression of the exogenous *MnSOD* cDNA was verified using the reverse transcriptase–polymerase chain reaction (RT-PCR) technique (51). One-microliter aliquots of reverse-transcribed cDNA were combined with 11 μl of a PCR solution consisting of 10 × PCR buffer, 0.63 U of *Taq* DNA polymerase (Boehringer Mannheim), 0.5 μ*M* dNTP, and

0.5 μl total of oligo primers. Two sets of oligo primers were used to distinguish endogenous from exogenous mRNA transcripts and are shown in Table 1. The first set of primers (CLONTECH) were 25-mers designed from the rat *MnSOD* cDNA sequence published by Ho and Crapo (10) and amplified a 383-bp PCR product representative of endogenous rat *MnSOD* transcript. To detect transcription of the exogenous mouse *MnSOD* cDNA, a 24-mer downstream primer was designed from the plasmid DNA sequence to include the last three bases of the EcoRI cloning site (3′ CTT <u>AAG</u> 5′) in the plasmid DNA sequence. This oligo was used in combination with the upstream primer from CLONTECH, which recognized the transfected mouse *MnSOD* cDNA at positions 218–242, whereas the downstream primer recognized the vector DNA starting at the AAG sequence of the *Eco*RI site. This combination of primers amplified a PCR product of 729-bp length, representative of exogenous *MnSOD* mRNA. PCR reactions were performed on a PerkinElmer Gene Amp PCR system 2400 under the following conditions: 35 cycles; T_{denat} = 94°C, 40 s; T_{anneal} = 55°C, 1 min; T_{exten} = 72°C, 1 min. The amplified products were electrophoresed at 70 V on a 2.0% agarose gel and photographed.

Activity gels

Antioxidant enzyme activity bands were visualized using native (nondenaturing) polyacrylamide gel electrophoresis (33, 46). SOD activity bands were resolved on 12% polyacrylamide gels (2, 22), whereas 8% polyacrylamide gels were used for resolution of CAT activity bands (47). Achromatic bands against a dark blue background represented SOD activity. CAT activity appeared as achromatic bands on a bright green background.

CAT activity

CAT activity was determined in whole cell homogenates according to the method of Beers and Sizer (3). In this assay, the disappearance of H_2O_2 was measured spectrophotometrically at 240 nm over a 60-s time interval. Because CAT displays unusual kinetics, k units rather than international units were used to report enzyme activity.

GPx activity

GPx was assayed according to a modified version of the method of Gunzler and Flohe (8). This assay entails the indirect, coupled measurement of GPx activity that is monitored by the disappearance of NADPH at 340 nm. Total and selenium-dependent (Se-dep) GPx were measured using cumene hydroperoxide and H_2O_2 (Sigma Chemical Co.), respectively, as substrates. One unit of GPx is defined as the amount of homogenate required for oxidation of 1 μmol of NADPH per minute.

Cell doubling time under serum restricted conditions

To evaluate cell doubling time(s) under serum restricted conditions, all cells were seeded in triplicate in 60-mm Corning tissue culture dishes at densities of 10^5 cells per dish. Cells were evaluated for growth rates at 10%, 5%, and 1% serum concentrations. Cell counts were obtained on a daily basis for 5 days using a Coulter counter, and plotted versus time to determine cell doubling time(s) in units of hours. Doubling time (DT) was calculated using

$$DT = 0.693t/\ln(N_t/N_0)$$

where t is the time in days, N_t is the cell number at time t, and N_0 is the cell number at the initial time.

Clonogenicity under serum restricted conditions

Cell plating efficiencies were calculated for 10%, 5%, and 1% serum concentrations. Cells were seeded in triplicate in 60-mm Corning tissue culture dishes at densities of 100 cells per dish for both 10% and 5% serum, and 200 cells per dish for 1% serum-supplemented cells. The cells were incubated for 14 days and then stained with crystal violet (Sigma Chemical Co.), and the colonies were counted. Plating efficiencies

TABLE 1. OLIGO PRIMER SEQUENCES USED IN RT-PCR REACTIONS TO DISTINGUISH ENDOGENOUS FROM EXOGENOUS MnSOD TRANSCRIPTS

Endogenous rat transcript specific oligo primer sequences (CLONTECH):
   Upstream 25-mer
      5′ GCG ACC TAC GTG AAC AAT CTG AAC G 3′ (177–202)
   Downstream 25-mer
      5′ TC AAT CCC CAG TGG AAT AAG GC 3′ (559–535)
      RT-PCR product: 383 bp

Exogenous transcript specific 3′ oligo primer sequence specific for vector DNA:
   Downstream 24-mer
      5′ TAT CTT ATC ATG TCT GGA TCG *GAA** 3′
   Upstream CLONTECH oligo recognition of mouse MnSOD cDNA
      5′ GCG <u>G</u>CC TAC GTG AAC AA<u>C</u> CT<u>C</u> AAC G 3′[†] (218–242)[‡]

*The last three italicized bases of the downstream 24-mer are specific for the *Eco*RI cloning site of the vector DNA.

[†]Underscoring denotes mismatched base pairing during recognition of the rat upstream 25-mer primer with the mouse MnSOD cDNA.

[‡]The 24-mer downstream primer was combined with the CLONTECH upstream primer (rat), which recognized the mouse cDNA at positions 218–242. This oligo combination amplified an RT-PCR product of 729 bp in length.

were calculated as the ratio of average colonies counted divided by the number of cells plated.

Clonogenicity in soft agar

Transfected and control populations grown in 10% serum were suspended at densities of 500–1,000 cells/ml in a final concentration of 0.35% agar and plated on top of a 0.5% agar nutrient layer to evaluate cellular anchorage independence (13). The cells were maintained at 37°C and 5% CO_2 for 2 weeks. Colonies were counted, and clonogenic fraction was calculated as described above.

Characterization of malignancy by injection in nude mice

Male nude mice (4 weeks old) were purchased from Harlan Sprague (Indianapolis, IN, U.S.A.) and were allowed to acclimate for 1 week prior to experiments. Control and MnSOD-overexpressing cell lines were injected subcutaneously in the right shoulder region at a titers of 5×10^6, 10^6, and 10^5 cells per 0.2-ml volume per animal, with $n = 4$ animals per group. All cells were suspended in serum-free Dulbecco's modified Eagle medium. Tumor volumes were measured every 3–4 days using a vernier caliper, for 30 days. Tumor volume (TV) was calculated by the following formula:

$$TV \ (mm^3) = (L \times W^2)/2$$

where L is the longest dimension of the tumor in millimeters and W is the shortest dimension of the tumor in millimeters (49, 50). The animals were killed by CO_2 asphyxiation, and then tumor and lung tissues were removed for fixation.

Light microscopic examination for metastases

Tissues were prepared for light microscopy by fixing in 10% buffered formalin for 2 h, then transferred to phosphate-buffered saline, pH 7.4, and embedded in paraffin. Sections were stained with hematoxylin and eosin and examined for metastases in a blinded fashion. Animals were scored positive for metastasis with the observation of at least one metastatic focus.

Statistical analysis

All data were analyzed using one-way ANOVA. Dunnett's test ($p \leq 0.05$) was used to determine any statistical significance of transfected populations when compared with the XR23M parental control. Scheffé's test was also used to compare differences among groups.

RESULTS

Isolation and screening of clones

Malignant rat XR23M cells were first transfected with a human *MnSOD* cDNA. We were able to isolate clones with increased MnSOD protein; however, these transfected cells demonstrated small increases in MnSOD enzymatic activity (data not shown). For this reason, the rat XR23M cells were

transfected with a mouse cDNA. Neomycin-resistant colonies were ring-isolated and maintained in culture for 6 weeks prior to characterization. The cells were screened for increased MnSOD immunoreactive protein by western blotting as shown in Fig. 1. Three clonal populations, mMn6, mMn9, and mMn185, demonstrated increases in immunoreactive MnSOD protein when compared with the parental XR23M control cell line. In addition, a fourth clone, mMn249, demonstrated decreased levels of immunoreactive protein when compared with the XR23M parental control, which is highly unusual and suggestive that disruption of *MnSOD* gene expression had occurred. MnSOD activity levels were measured in all cell lines to verify that the overexpressed protein was correctly processed to make active enzyme. The enzymatic activity levels are presented in Table 2. When compared with the XR23M parental control, MnSOD activity of mMn6, mMn9, and mMn185 was approximately three- to fivefold increased, whereas mMn249 was approximately fourfold decreased; these activities are consistent with the immunoreactive protein levels shown in Fig. 1.

Southern analysis of *Eco*RI-digested DNA shown in Fig. 2 demonstrates stable incorporation of the mouse cDNA into the genome of the *MnSOD*-transfected cell lines. The endogenous *MnSOD* gene was characterized in the parental and vector controls (lanes 2–4) by two bands migrating at approximately 9.4 and 6.5 kb. In addition to these two migrating fragments, a multiband pattern was observed in all *MnSOD*-transfected populations. The smallest fragment migrated at 0.8 kb and is consistent in length with the 0.8-kb transfected *MnSOD* cDNA. In addition, slower migrating fragments were observed in the *MnSOD*-transfected cell lines only. These fragments may be a reflection of incomplete digestion of the plasmid DNA. These data verify that the neomycin-resistant cells had incorporated the *MnSOD* cDNA into the host genome.

Next, primer sequences were designed (Table 1) to demonstrate transcription of the transfected cDNA and to distinguish exogenous from endogenous message. Primers (CLONTECH) designed from the rat *MnSOD* cDNA sequence were used for the detection of endogenous transcript in the XR23M rat cells (10). These primers amplified an RT-PCR product characterized by a calculated length of 383 bp. To discern ex-
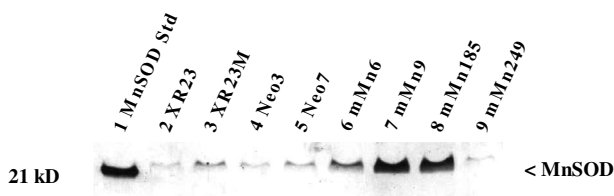

FIG. 1. Western analysis of control and MnSOD-overexpressing cell lines. Sample lanes contained 20 μg of protein. Lane 1, 0.5 μg of purified human kidney MnSOD; lane 2, XR23 nonmalignant control; lane 3, parental XR23M malignant control; lane 4, Neo3 vector control; lane 5, Neo7 vector control; lane 6, mMn6; lane 7, mMn9; lane 8, mMn185; lane 9, mMn249. Immunoreactive protein was probed with human kidney MnSOD antibody diluted 1:1,250.

TABLE 2. ANTIOXIDANT ENZYME PROFILE OF XR23M MALIGNANT CONTROL, VECTOR CONTROL, AND MnSOD OVEREXPRESSORS

Clone	Total SOD	MnSOD	CuZnSOD	CAT	Total GPx	Se-dep GPx
XR23	NM	NM	NM	12 ± 1.0*	NM	3.99 ± 0.99
XR23M	444 ± 96	23 ± 3	421 ± 94	18 ± 1.0	5.99 ± 2.27	4.03 ± 1.33
Neo3	217 ± 23*	14 ± 2	203 ± 21*	41 ± 3.0*	5.81 ± 0.66	4.54 ± 0.54
Neo7	317 ± 27	28 ± 3	289 ± 30	6 ± 1.0*	4.57 ± 0.15	4.36 ± 0.15
mMn6	500 ± 0	66 ± 22*	434 ± 22	18 ± 2.0	5.36 ± 0.58	4.69 ± 0.58
mMn9	467 ± 58	92 ± 2*	375 ± 57	30 ± 2.0*	4.01 ± 0.63	5.07 ± 0.16
mMn185	361 ± 127	101 ± 31*	260 ± 142	6 ± 0.5*	3.11 ± 0.51*	3.51 ± 0.99
mMn249	156 ± 20*	6 ± 2	150 ± 19*	15 ± 1.0	4.21 ± 1.14	3.11 ± 0.26

SOD activity is reported as U/mg of protein ± SD. CAT activity is reported as k/g of protein ± SD. GPx activity is reported as mU/mg of protein ± SD. NM, not measured.

*Significantly different compared with XR23M parental control at $p \leq 0.05$.

ogenous transcript from the mouse cDNA insert, the upstream primer from CLONTECH was combined with a primer designed to specifically recognize the *Eco*RI insertion site of the plasmid DNA sequence, which contained the *MnSOD* cDNA. This combination of primers amplified an RT-PCR product of 729 bp calculated length. Figure 3 illustrates the results of the RT-PCR assay. Exogenous and endogenous transcripts are shown in lanes 1–9 and 11–19, respectively. Lanes 1 and 19 contained RT-PCR product amplified from the *MnSOD* cDNA plasmid in combination with the respective primers, whereas lane 10 contained molecular weight markers. Lanes 2–5 and 11–14 contained product of the parental and vector controls, whereas lanes 6–9 and 15–18 contained RT-PCR product of the *MnSOD* cDNA transfected cell lines. Lanes 6–8 demonstrate the active transcription of exogenous cDNA

in mMn6, mMn9, and mMn185 MnSOD overexpressors as characterized by the 693-bp amplified transcript. Lanes 11–18 show RT-PCR product of the endogenous *MnSOD* gene in all cell lines. Interestingly, mMn249 demonstrated transcription of the endogenous *MnSOD* gene, whereas that of the exogenous *MnSOD* cDNA was not detectable. Thus, clone mMn249 is not producing RNA from the plasmid, and this is consistent with the lowered MnSOD protein observed. Based on sequence information, the calculated lengths of the exogenous (729 bp) and endogenous (383 bp) RT-PCR products were reasonably consistent with the 693- and 404-bp products resolved on the gel as sequence calculations and gel resolution measurements were within 5% for both endogenous and exogenous amplimers.

Effects of MnSOD modulation on other antioxidant proteins

Next, we studied the affect of overexpression of MnSOD on the levels of other antioxidant enzymes via western blotting, activity gels, and activity assays. Figure 4 shows the western analyses of CuZnSOD and CAT in MnSOD-overexpressing cells. Staining intensities for CuZnSOD were similar among XR23M parental and vector controls, as well as mMn6 and mMn9, but were slightly lower in mMn185 and mMn249. Figure 4B demonstrates some variation in the 60-kDa immunoreactive CAT protein, as mMn185 and mMn249 contain less immunoreactive CAT when compared with the XR23M parental control. In addition to the 60-kDa CAT subunit, a 30-kDa faster migrating subunit was also observed, and is consistent with other published reports (42). Western blotting was performed with GPx antibody, but multiple bands were seen, and so these data were not interpretable.

Enzymatic activity levels of CuZnSOD and CAT were determined by both activity gels and spectrophotometric assay. Figure 5A demonstrated similar CuZnSOD activity as determined by activity gel among control and transfected populations. CAT activity gel analysis demonstrated some variation, as mMn9 appeared to be higher and Neo7 and mMn185 were lower when compared with parental XR23M, as shown in Fig. 5B. CAT and GPx enzymatic activity levels were also measured spectrophotometrically in all cell lines to complete the antioxidant enzyme profile, and are summarized along with SOD activity levels in Table 2. When compared with the
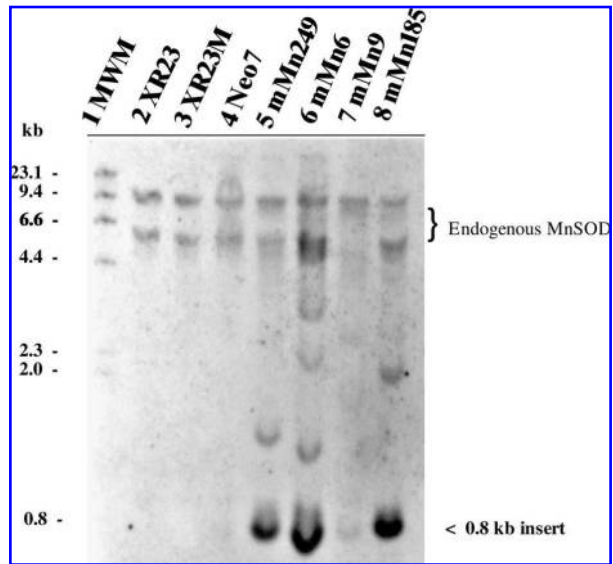

FIG. 2. **Southern blot analysis of parental and vector controls and *MnSOD*-transfected cell lines.** Each lane contained 30 μg of *Eco*RI-digested DNA. Lane 1, digoxigenin-labeled molecular weight markers; lane 2, XR23 nonmalignant control; lane 3, XR23M malignant control; lane 4, Neo7 vector control; lane 5, mMn249; lane 6, mMn6; lane 7, mMn9; lane 8, mMn185.
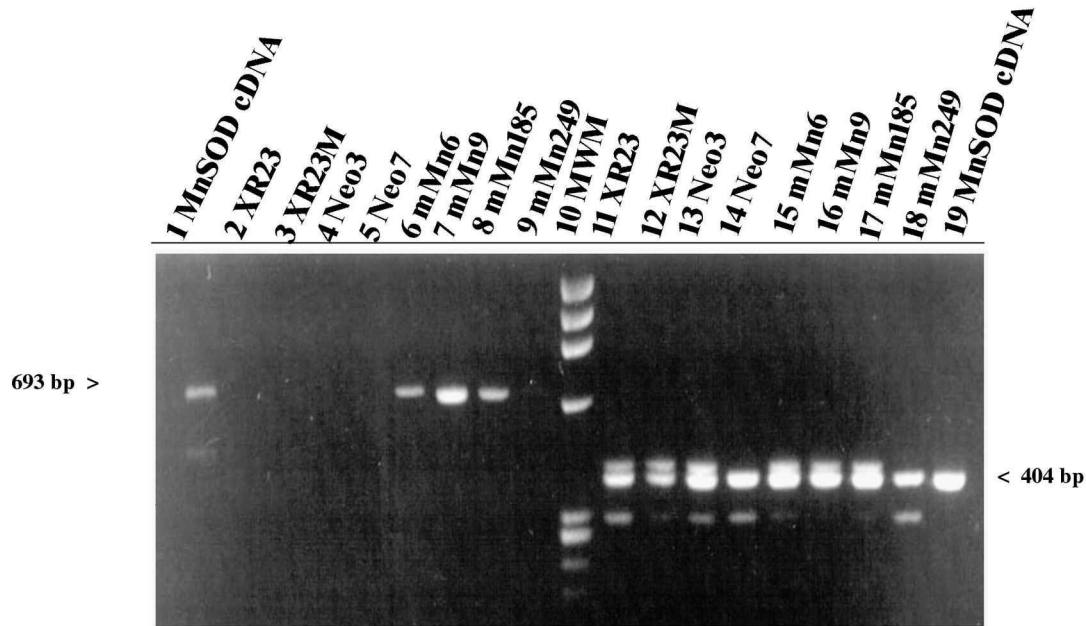
FIG. 3. RT-PCR analysis of parental and vector controls and *MnSOD*-transfected cell lines. Lanes 1–9 contained RT-PCR product of exogenous transcript, whereas lanes 11–19 contained RT-PCR product from endogenous transcript. Each lane contained 10 μl of RT-PCR product in the following order: lane 1, *MnSOD* cDNA control; lane 2, XR23 nonmalignant control; lane 3, XR23M malignant control; lane 4, Neo3 vector control; lane 5, Neo7 vector control; lane 6, mMn6; lane 7, mMn9; lane 8, mMn185; lane 9, mMn249; lane 10, molecular weight markers; lane 11, XR23 nonmalignant control; lane 12, XR23M malignant control; lane 13, Neo3 vector control; lane 14, Neo7 vector control; lane 15, mMn6; lane 16, mMn9; lane 17, mMn185; lane 18, mMn249; lane 19, *MnSOD* cDNA control.

parental XR23M cell line, total SOD and CuZnSOD activity levels were similar in all clonal populations with the exception of Neo3 vector control and mMn249, the clonal population that demonstrated the lowest levels of MnSOD activity. MnSOD activity was significantly increased in mMn6, mMn9, and mMn185 and is consistent with immunoreactive protein levels shown in Fig. 1. CAT activity levels in mMn6 demonstrated no difference, whereas mMn9 was 1.7-fold increased and mMn185 was 2.7-fold decreased when compared with the XR23M parental control. Se-dep GPx activities demon-

strated no significant variation; however, total GPx activity in mMn185 was significantly less than the XR23M parental control activity levels. Because transfected cells exhibited some variation in peroxide metabolizing enzymes, MnSOD: CAT and MnSOD:GPx activity ratios of the control and transfected cell lines were calculated to evaluate the possibility of antioxidant imbalance and are summarized in Table 3. In general, MnSOD overexpressors exhibited higher MnSOD:CAT and MnSOD:GPx ratios when compared with control populations, whereas the MnSOD underexpressor, mMn249, exhib-
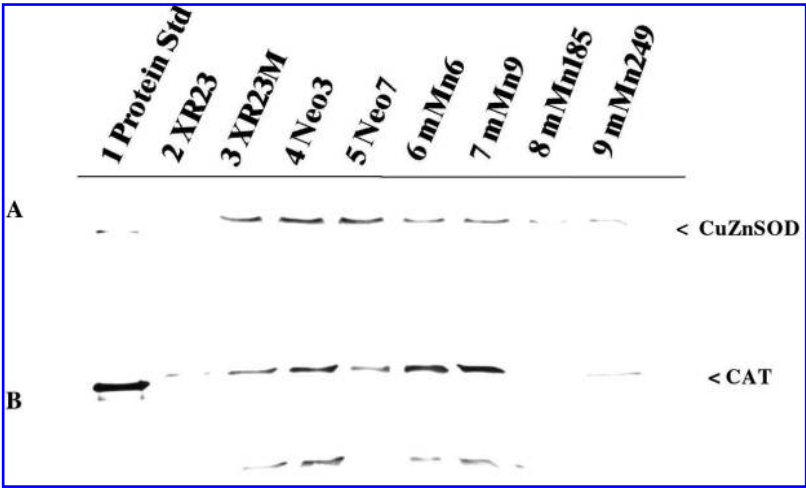

FIG. 4. Western analysis of control and MnSOD-overexpressing cell lines. Sample lanes contained 20 μg of protein. Lane 1, 0.5 μg of purified enzyme standard; lane 2, XR23 nonmalignant control; lane 3, parental XR23M malignant control; lane 4, Neo3 vector control; lane 5, Neo7 vector control; lane 6, mMn6; lane 7, mMn9; lane 8, mMn185; lane 9, mMn249. Immunoreactive protein was probed with human rCuZnSOD and human erythrocyte CAT antibodies diluted 1:500. The purified enzyme standards were bovine CuZnSOD and bovine liver CAT.

FIG. 5. Native activity gel analysis of (A) CuZnSOD and (B) CAT enzymes in control and MnSOD-overexpressing cell lines. Sample lanes contained 50 μg of protein. Lane 1, purified enzyme standard (10 μg of bovine CuZnSOD or 0.13 μg of human erythrocyte CAT); lane 2, XR23 nonmalignant control; lane 3, parental XR23M malignant control; lane 4, Neo3 vector control; lane 5, Neo7 vector control; lane 6, mMn6; lane 7, mMn9; lane 8, mMn185; lane 9, mMn249.
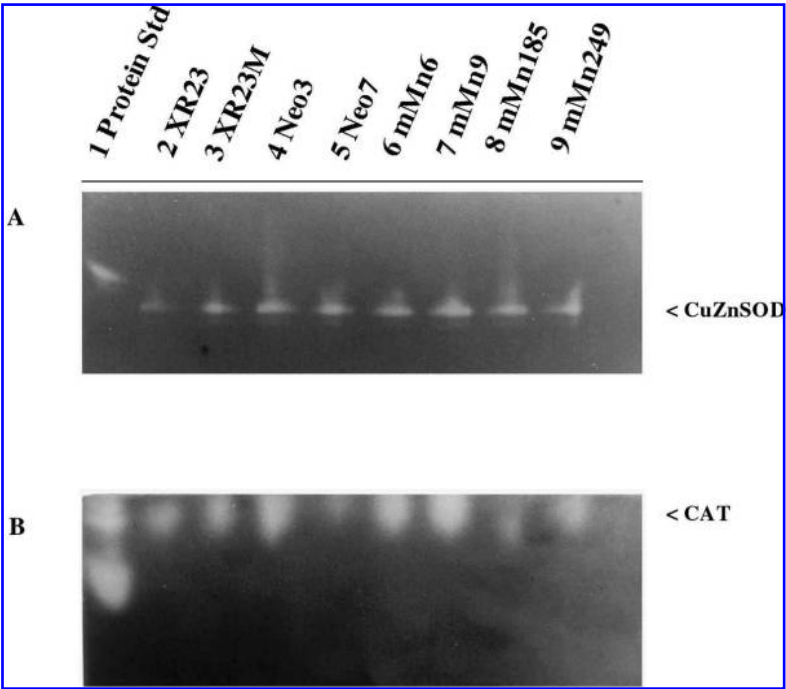
ited lower MnSOD:CAT and MnSOD:GPx ratios. These results demonstrate an antioxidant imbalance (peroxide-generating versus peroxide-metabolizing enzymes) in the *MnSOD*-transfected cell lines.

Next, the effect of MnSOD overexpression on *in vitro* and *in vivo* growth was investigated. To accomplish this, the following analyses were performed: (a) *in vitro* evaluations of cell doubling times, plating efficiencies, and anchorage-independent growth in soft agar, and (b) tumor growth and lung metastasis in nude mice. When compared with the XR23M parental control, MnSOD overexpressors demonstrated a 1.5–2-fold increase in cell doubling times when grown in 1% serum (data not shown). MnSOD overexpressors formed no countable colonies when grown in 1% serum, whereas the plating efficiency of the XR23M parental control was 4% (data not shown). Similarly, when plated in soft agar, the XR23M parental and Neo3 vector control cell lines demonstrated 6.8% and
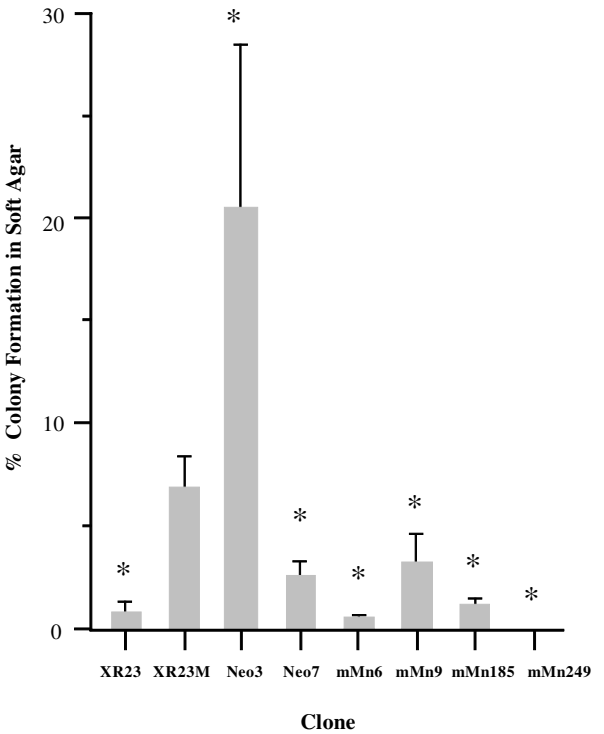
TABLE 3. RATIOS OF PEROXIDE-GENERATING:
PEROXIDE-METABOLIZING ENZYMES IN CONTROL
AND MnSOD OVEREXPRESSORS

Clone	MnSOD: CAT	MnSOD: total GPx	MnSOD: Se-dep GPx
XR23M	1.3	3.8	5.7
Neo3	0.3	2.4	3.1
Neo7	4.7	6.1	6.4
mMn6	3.7	12.3	14.1
mMn9	3.1	22.9	18.2
mMn185	16.8	32.5	28.8
mMn249	0.4	1.4	1.9

Ratios were calculated from data presented in Table 2.

FIG. 6. The effects of MnSOD overexpression on clonogenicity in soft agar. *Significantly different from XR23M at the $p < 0.05$ level. No colony formation was observed in clone mMn249.

20.5% colony-forming abilities, respectively, whereas MnSOD overexpressors formed colonies ranging from 0% to 3.2% (Fig. 6). These results are expected because, in general, cancer cells show a higher frequency of growth in soft agar than normal cells. These studies demonstrate that MnSOD overexpression has inhibitory effects on the *in vitro* growth of cells grown in 1% serum or in 10% serum and 0.35% soft agar.

The *in vivo* growth effects of MnSOD overexpression on tumor-forming ability and rate of metastasis to the lung in nude mice were also evaluated. Three to four animals per cell line were used, and each experiment varied according to the number of cells injected per animal, as well as the duration of the experiment. Figure 7A demonstrates tumor formation of the three MnSOD-overexpressing cells (mMn6, mMn9, and mMn185) when compared with the XR23M parental control. One million cells were injected per animal in this experiment.

Tumor growth was apparent by day 14, at which point tumor volumes were measured over a period of 30 days. When compared with the parental XR23M cell line, MnSOD overexpressors exhibited reduced tumor volume as MnSOD activity increased (see Table 2). Moreover, an average of 10.5 lung metastases per animal were quantified for the XR23M malignant control, whereas 0.5–1.5 were quantified in lung tissue derived from animals injected with MnSOD-overexpressing cells (Fig. 7B). Also, metastatic potential demonstrated a linear response with respect to MnSOD activity levels, with a linear regression correlation coefficient of −0.94 (Fig. 7B inset and Table 4). Similar growth kinetics was observed in two additional experiments, in which 1×10^5 or 5×10^6 cells were injected per animal (data not shown).

The most interesting observation of the effects of *MnSOD* transfection on *in vivo* tumor growth pertained to the unantic-
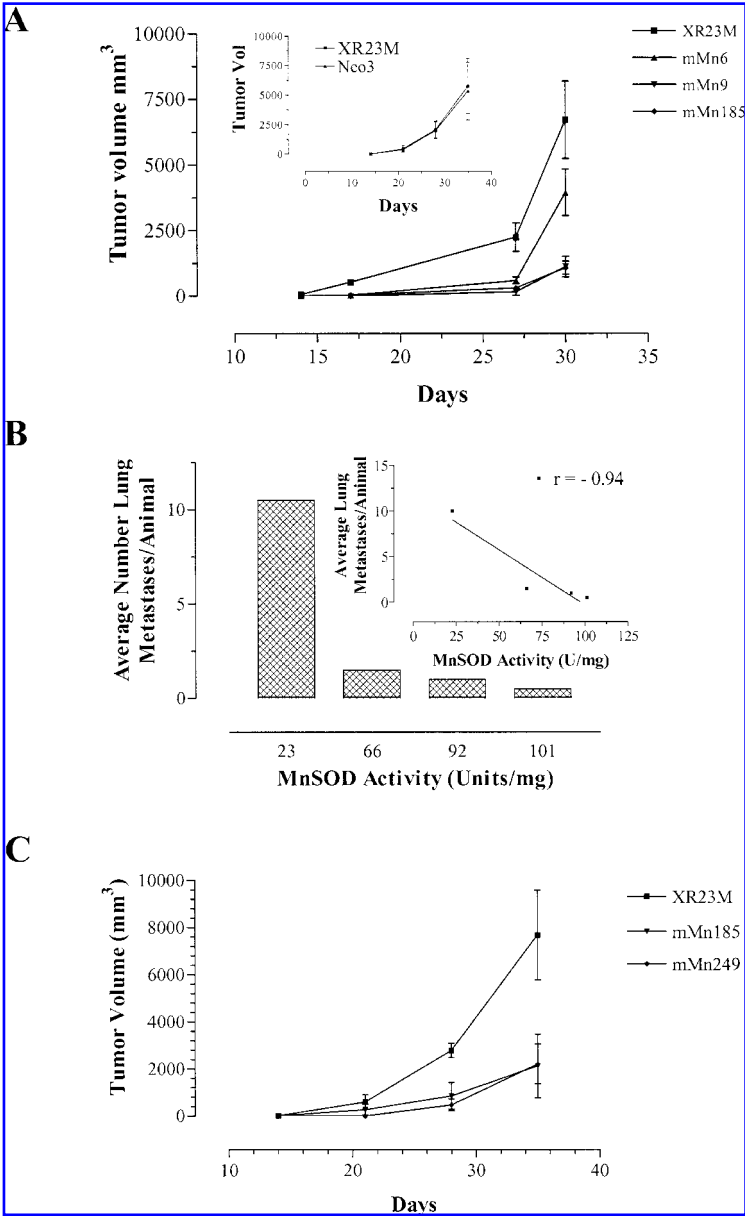

FIG. 7. **(A)** *In vivo* growth rates of MnSOD overexpressors compared with XR23M malignant control. One million cells were injected per animal. Mean tumor volumes were calculated from four animals. The **inset** figure demonstrates similar growth rates of the Neo3 vector control and parental XR23M cell line; in this experiment, 10^5 cells were injected per animal. **(B)** *In vivo* effects of MnSOD overexpression on metastatic potential in XR23M parental control, mMn6, mMn9, and mMn185 cell lines, which exhibit two- to fourfold increases in MnSOD activity when compared with XR23M control. The **inset** demonstrates the linearity of the association between MnSOD activity and metastatic potential. **(C)** *In vivo* growth rates of mMn249 (fourfold MnSOD underexpressor) and mMn185 (fourfold MnSOD overexpressor) compared with XR23M parental control. Cells (1×10^5) were implanted in the shoulders of each animal. Tumor growth was followed in three (XR23M and mMn249) or four (mMn185) animals for 35 days.

TABLE 4. SUMMARY OF LINEAR REGRESSION CORRELATION COEFFICIENTS RELATING METASTATIC POTENTIAL TO ANTIOXIDANT PROFILE, AS WELL AS COMPARING THE OTHER ANTIOXIDANT ENZYME ACTIVITIES TO MnSOD ACTIVITY

	Linear regression (r)
Metastatic potential* vs. MnSOD activity†	−0.9458
Metastatic potential vs. MnSOD:GPx‡	−0.8248
Metastatic potential vs. MnSOD:CAT‡	−0.5685
Metastatic potential vs. total GPx activity†	0.7613
MnSOD activity vs. total GPx activity†	−0.9348

*Metastatic potential was based on values presented in Fig. 7.
†MnSOD and total GPx activity levels are presented in Table 2.
‡MnSOD:GPx and MnSOD:CAT ratios are presented in Table 3.

ipated, slower *in vivo* growth of clone mMn249, which underexpressed MnSOD when compared with the XR23M control (Fig. 7C). In light of this finding, the *in vivo* data were analyzed relative to each cell line antioxidant profile (Tables 2 and 3). To this end, Fig. 8 demonstrates tumor volume plotted as a function of (A) MnSOD activity and (B) MnSOD:Se-dep GPx ratio. The shapes of these curves are provocative and suggest an involvement of antioxidant imbalance in the suppression of tumor growth in transfected cell lines that both underexpress and overexpress MnSOD. Moreover, these data suggest an optimum antioxidant/oxidant level, which may be necessary for proliferation of the tumor cell. To this end, linear regression correlation coefficients were calculated relative to metastatic potential (Fig. 7B inset) and antioxidant profile (Tables 2 and 3), and are summarized in Table 4. Linear regression analyses of these data suggest that metastatic potential decreases linearly as a function of the following parameters: increased MnSOD activity, decreased total GPx activity, increased MnSOD:CAT ratios, and increased MnSOD: total GPx ratios, and is suggestive of a role of increased intracellular peroxides in the antimetastatic effects of MnSOD overexpression. It should be pointed out here that although fewer metastases were observed in the animals injected with MnSOD overexpressing clones, these clones also grew much more slowly. So, one possibility is that the metastases were fewer simply because the primary tumors were smaller. Further experiments are necessary to examine this question. In summary, these results suggest that MnSOD overexpression suppresses tumor growth, as well as metastasis to the lung, and that these anticancer effects may be mediated through alterations in the balance between peroxide-generating versus peroxide-metabolizing enzymes within the tumor.

DISCUSSION

MnSOD has been shown to function as an antitumor agent (25). The current report demonstrates growth inhibitory effects in *MnSOD* transfectants that overexpress active enzyme. We could only obtain clones that had increased MnSOD activity when we transfected with mouse *MnSOD* cDNA and not
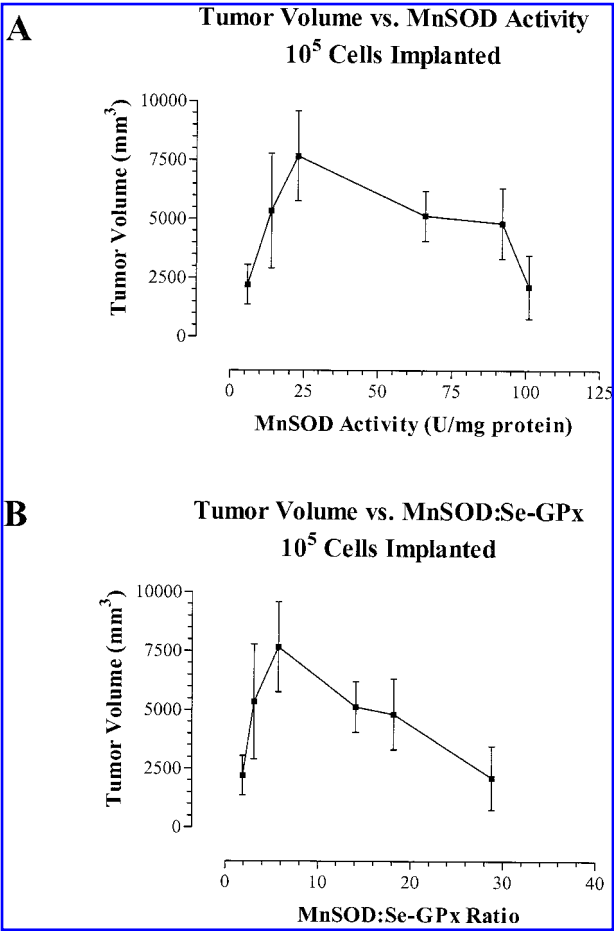
FIG. 8. Tumor volume as a function of (A) MnSOD activity and (B) MnSOD:Se-dep GPx ratio. Tumor volumes were obtained from animals injected with 10^5 cells, whereas MnSOD activity and MnSOD:Se-dep GPx ratios were taken from Tables 2 and 3, respectively.

human *MnSOD* cDNA. We have obtained this result in other rat cell lines also. These results suggest that cross-species transfections with *MnSOD* cDNA should be done with caution.

Interestingly, one clonal population that underexpressed the MnSOD enzyme also exhibited tumor suppressive effects. Why this clone underexpressed MnSOD remains a mystery, but is most likely due to integration of the transfected cDNA into a region of the rat genome that affects MnSOD expression. This result was based on only one clone, and so more clones need to be investigated to firm up this observation. Nevertheless, the results suggest that inhibition of MnSOD could also be utilized as a growth inhibitory strategy for cancer. This could be done with antisense oligos or small interfering RNA.

We hypothesize that the tumor suppressive effects for both the over- and underexpressors may be explained by alterations in antioxidant balance within the transfected cell lines, which in this study is characterized by the ratios of peroxide-generating to peroxide-metabolizing enzyme activities. In support of this hypothesis, Li *et al.* have isolated clonal populations of human DU145 prostate carcinoma cells overex-

pressing MnSOD, which were characterized as adapted (two-fold increase in MnSOD and twofold increase in CAT) and nonadapted (fivefold increase in MnSOD with no measurable change in CAT) (15, 16). When compared with that of parental controls, electron microscopic analysis of nonadapted cells only, demonstrated mild focal loss of mitochondrial cristae under normal cell culture conditions, whereas dramatic mito-chondrial injury was observed following exposure to 1.5 mM H_2O_2. Both adapted and nonadapted cell lines demonstrated an accumulation of intracellular peroxides that were associated with a slight decrease in cell viability. However, when compared with parental and vector controls, exposure to exogenous H_2O_2 or mitomycin C resulted in decreased viability of the nonadapted clone only (15). In addition, decreased glutathione (GSH):glutathione disulfide (GSSG) ratios were associated with cell cycle alterations in the adapted and nonadapted cell lines (16). These results demonstrate that overexpression of MnSOD perturbs the intracellular antioxidant balance, which under specific growth conditions leads to an accumulation of intracellular peroxides at least in the mitochondria and decreased cell viability.

The suggestion of a role of antioxidant or redox imbalance in the anticancer effects of MnSOD has been suggested in other reports. For example, overexpression of MnSOD (5.7-fold) in MCF-7 malignant breast cancer cells resulted in a nonproliferating clonal population, which remained quiescent unless 10 mM pyruvate, a H_2O_2 scavenger, was added to the tissue culture media (14). More recent studies have demonstrated that the growth inhibitory effects of MnSOD overexpression are mediated by the generation of intracellular peroxides. To this end, the overexpression of either GPx or CAT reversed the growth inhibitory effects of MnSOD by altering the intracellular redox status (17, 37). Moreover, Kim *et al.* have demonstrated that tumor cell growth inhibition mediated by MnSOD overexpression was associated with increased aconitase activity, decreased intracellular GSH:GSSG ratio, and a dose-dependent inhibition of pyruvate carboxylase activity (11). These results demonstrated that MnSOD-mediated alterations in the steady-state concentrations of mitochondrial $O_2^{\cdot-}$ and H_2O_2 impact cellular metabolic capacity, culminating in inhibitory effects on tumor cell proliferation (11). In another report, MnSOD-mediated suppression of tumor growth was enhanced by the glutathione reductase inhibitor 1,3-bis(2-chloroethyl)-1-nitrosourea (BCNU), and the GSH synthesis inhibitor buthionine sulfoximine (49). Moreover, the sensitivity to BCNU-mediated cell killing was partially inhibited by pyruvate, a H_2O_2 scavenger, further implicating an involvement of peroxides in the tumor suppressive effects of MnSOD overexpression. These results support the hypothesis that the antitumor effects of MnSOD are mediated at least in part through alterations in intracellular antioxidant/redox balance leading to conditions that are unfavorable for tumor growth.

The concept of antioxidant imbalance may also explain the observation in the current report, pertaining to the antiproliferative effect of MnSOD underexpression on tumor growth in a selected clonal population. When compared with the XR23M control, underexpression (fourfold decrease) as well as overexpression (fourfold increase) of MnSOD resulted in reduced tumor growth (Fig. 8A). The same pattern of growth inhibition was observed when tumor volume was plotted as a

function of MnSOD:Se-dep GPx ratio (Fig. 8B). MnSOD:Se-dep GPx ratio is a measure of enzymatic activities involved in H_2O_2 generation versus H_2O_2 metabolism, and therefore suggests a role of H_2O_2 in tumor cell growth. This ratio increased linearly as a function of MnSOD overexpression and was associated with tumor growth inhibition in three of the selected populations. However, a sharp decrease in MnSOD activity and MnSOD:Se-dep GPx ratio (mMn249) was also associated with growth inhibition and suggests a requirement of an optimum level of H_2O_2 for tumor cell growth as shown in Fig. 8. The involvement of H_2O_2 concentration dependence in the regulation of cellular response has been reviewed by Davies (6) and may explain these results. In this review, very low levels of H_2O_2 (3–15 μM) elicit a significant mitogenic response resulting in 25–45% stimulation of growth, whereas higher levels (120–150 μM) cause temporary growth arrest, followed by an adaptive stress response in which protective proteins are induced. At H_2O_2 concentrations of 250–400 μM, permanent growth arrest occurs in cells, which otherwise maintain what appears to be normal cellular function. Further increases in H_2O_2 concentration ($\geq$1 mM) result in apoptosis and necrosis (6).

One factor that must be taken into account in the discussion of the effects of MnSOD modulation is cell location. MnSOD is a mitochondrial protein and is thought to be enzymatically active only in the mitochondria. The Se-dep GPx that our assay measures is probably mostly cytosolic GPx or GPx1. This GPx is found in the cytoplasm, nucleus, and mitochondria. On the other hand, CAT is found mostly in peroxisomes and sometimes in the cytoplasm. Thus, the increased peroxides that we and others have alluded to probably occur in the mitochondria first and may diffuse to the cytoplasm. GPx1 is in a good location to remove these peroxides, but CAT and other peroxide-removing proteins may not be as effective due to their removed location.

In summary, the results in this study demonstrate MnSOD-mediated growth inhibition and antimetastatic effects in XR23M tumor cells, which are associated with alterations in antioxidant balance. These data also suggest the requirement of an optimal balance between intracellular oxidants and antioxidants for tumor cell growth, and are supportive of the hypothesis that the critical factor distinguishing normal cell division from that of transformed cells involves the intracellular levels of H_2O_2 (27). These results were found in fibroblasts, and it remains to be seen if similar results would be observed in epithelial cells, which are the source of the majority of human cancers.

ACKNOWLEDGMENTS

ABBREVIATIONS

BCNU, 1,3-bis(2-chloroethyl)-1-nitrosourea; CAT, catalase; CuZnSOD, copper- and zinc-containing superoxide dismutase; GPx, glutathione peroxidase; GSH, glutathione;

GSSG, glutathione disulfide; H_2O_2, hydrogen peroxide; MnSOD, manganese-containing superoxide dismutase protein; *MnSOD*, manganese-containing superoxide dismutase gene, cDNA, or RNA; NBT, nitro blue tetrazolium; $O_2^{\cdot-}$, superoxide radical; PCR, polymerase chain reaction; ROS, reactive oxygen species; RT-PCR, reverse transcriptase–polymerase chain reaction; Se-dep, selenium-dependent; SOD, superoxide dismutase.

REFERENCES

1. Angel P, Imagawa M, Chiu R, Stein B, Imbra RJ, Rahmsdorf HJ, Jonat C, Herrlich P, and Karin M. Phorbol ester-inducible genes contain a common *cis* element recognized by a TPA-modulated *trans*-acting factor. *Cell* 49: 729–739, 1987.

2. Beauchamp C and Fridovich I. Superoxide dismutases: improved assays and an assay applicable to polyacrylamide gel. *Anal Biochem* 44: 276–287, 1971.

3. Beers RF Jr and Sizer IW. A spectrophotometric method for measuring the breakdown of hydrogen peroxide by catalase. *J Biol Chem* 195: 133–140, 1952.

4. Bravard A, Sabatier L, Hoffschir F, Luccioni C, and Dutrillaux B. SOD2: a new type of tumor suppressor gene? *Int J Cancer* 51: 475–480, 1992.

5. Church SL, Grant JW, Ridnour LA, Oberley LW, Swanson PE, Meltzer PS, and Trent JM. Increased manganese superoxide dismutase expression suppresses the malignant phenotype of human melanoma cells. *Proc Natl Acad Sci U S A* 90: 3113–3117, 1993.

6. Davies KJ. The broad spectrum of responses to oxidants in proliferating cells: a new paradigm for oxidative stress. *IUBMB Life* 48: 41–47, 1999.

7. Gille JJ, van Berkel CG, and Joenje H. Mutagenicity of metabolic oxygen radicals in mammalian cell cultures. *Carcinogenesis* 15: 12695–12699, 1994.

8. Gunzler WA and Flohe L. Glutathione peroxidase. In: *Handbook of Methods for Oxy Radical Research*, edited by Greenwald RA. Boca Raton, FL: CRC Press, 1985, pp. 285–290.

9. Halliwell B and Gutteridge JMC. *Free Radicals in Biology and Medicine*, 2nd edit. Oxford: Clarendon Press, 1989.

10. Ho YS and Crapo JD. Nucleotide sequences of cDNAs coding for rat manganese-containing superoxide dismutase. *Nucleic Acids Res* 15: 10070, 1987.

11. Kim KH, Rodriguez AM, Carrico PM, and Melendez JA. Potential mechanisms for the inhibition of tumor cell growth by manganese superoxide dismutase. *Antioxid Redox Signal* 3: 361–373, 2001.

12. Kiningham KK and St. Clair DK. Overexpression of manganese superoxide dismutase selectively modulates the activity of Jun-associated transcription factors in fibrosarcoma cells. *Cancer Res* 57: 5265–5271, 1997.

13. Li JJ and Dewey WC. Relationship between thermal tolerance and protein degradation in temperature-sensitive mouse cells. *J Cell Physiol* 151: 310–317, 1992.

14. Li JJ, Oberley LW, St. Clair DK, Ridnour LA, and Oberley TD. Phenotypic changes induced in human breast cancer cells by overexpression of manganese-containing superoxide dismutase. *Oncogene* 10: 1989–2000, 1995.

15. Li N, Oberley TD, Oberley LW, and Zhong W. Overexpression of manganese superoxide dismutase in DU145 human prostate carcinoma cells has multiple effects on cell phenotype. *Prostate* 35: 221–233, 1998.

16. Li N, Zhai Y, and Oberley TD. Two distinct mechanisms for inhibition of cell growth in human prostate carcinoma cells with antioxidant enzyme imbalance. Free *Radic Biol Med* 26: 1554–1568, 1999.

17. Li S, Yan T, Yang JQ, Oberley TD, and Oberley LW. The role of cellular glutathione peroxidase redox regulation in the suppression of tumor cell growth by manganese superoxide dismutase. *Cancer Res* 60: 3927–3939, 2000.

18. Liang BC, Ross DA, Greenburg HS, Meltzer PS, and Trent JM. Evidence for allelic imbalance of chromosome 6 in human astrocytomas. *Neurology* 44: 533–536, 1994.

19. Liu R, Oberley TD, and Oberley LW. Transfection and expression of MnSOD cDNA decreases tumor malignancy of human oral squamous carcinoma SCC-25 cells. *Hum Gene Ther* 8: 585–595, 1997.

20. Lowry OH, Rosebrough NJ, Farr AL, and Randall AL. Protein measurement with the Folin phenol reagent. *J Biol Chem* 193: 265–275, 1951.

21. Makarov SS, Jonat C, and Haskill S. Hyperinducible human metallothionein promoter with a low level basal activity. *Nucleic Acids Res* 22: 1504–1505, 1994.

22. McCormick ML, Oberley TD, Elwell JH, Oberley LW, Sun Y, and Li JJ. Superoxide dismutase and catalase levels during estrogen-induced renal tumorigenesis, in renal tumors and their autonomous variants in the Syrian hamster. *Carcinogenesis* 12: 977–983, 1991.

23. Millikin D, Meese E, Vogelstein B, Witkowski C, and Trent JM. Loss of heterozygosity for the long arm of chromosome 6 in human malignant melanoma. *Cancer Res* 51: 5449–5453, 1991.

24. Mylonas C and Kouretas D. Lipid peroxidation and tissue damage (review). *In Vivo* 13: 295–309, 1999.

25. Oberley LW. Anticancer therapy by overexpression of superoxide dismutase. *Antioxid. Redox Signal* 3: 461–472, 2001.

26. Oberley LW and Buettner GR. Role of superoxide dismutase in cancer: a review. *Cancer Res* 39: 1141–1149, 1979.

27. Oberley LW, Oberley TD, and Buettner GR. Cell division in normal and transformed cells: the possible role of superoxide and hydrogen peroxide. *Med Hypotheses* 7:21–42, 1981.

28. Oberley LW, McCormick ML, Sierra-Rivera E, and Kasemset-St. Clair D. Manganese superoxide dismutase in normal and transformed human embryonic lung fibroblasts. *Free Radic Biol Med* 6: 379–384, 1989.

29. Oberley TD and Oberley LW. Oxygen radicals and cancer. In: *Free Radicals in Aging*, edited by Yu BP. Boca Raton, FL: CRC Press, 1993, p. 247.

30. Oberley TD, Oberley LW, Slattery AF, Lauchner LJ, and Elwell JH. Immunohistochemical localization of antioxidant enzymes in adult Syrian hamster tissues and during kidney development. *Am J Pathol* 137: 199–214, 1990.

31. Oberley TD, Oberley LW, Slattery AF, and Elwell JH. Immunohistochemical localization of glutathione-*S*-transferase and glutathione peroxidase in adult Syrian hamster tissues and during kidney development. *Am J Pathol* 139: 355–369, 1991.

32. Oberley TD, Coursin DB, Cihla HP, Oberley LW, El-Sayad N, and Ho YS. Immunolocalization of manganese superoxide dismutase in normal and transgenic mice expressing the human enzyme. *Histochem J* 25: 267–279, 1993.

33. Ornstein L. Disc electrophoresis I: background and theory. *Ann N Y Acad Sci* 121: 321–349, 1964.

34. Piotr C and Nicoletta S. Single-step method of RNA isolation by acid guanidinium thiocyanate–phenol–chloroform extraction. *Anal Biochem* 162: 156–159, 1987.

35. Reardon DA, Entrekin RE, Sublett J, Ragsdale S, Li H, Boyett J, Kepner JL, and Look AT. Chromosome arm 6q loss is the most common recurrent autosomal alteration detected in primary pediatric ependymoma. *Genes Chromosomes Cancer* 24: 230–237, 1999.

36. Ridnour LA. MnSOD overexpression suppresses tumor growth and decreases metastatic potential in a malignant rat cell line. Doctoral Thesis, University of Iowa, 1995.

37. Rodriguez AM, Carrico PM, Mazurkiewicz JE, and Melendez JA. Mitochondrial or cytosolic catalase reverses the MnSOD-dependent inhibition of proliferation by enhancing respiratory chain activity, net ATP production, and decreasing the steady state levels of H_2O_2. *Free Radic Biol Med* 29: 801–813, 2000.

38. Safford SE, Oberley TD, Urano M, and St. Clair DK. Suppression of fibrosarcoma metastasis by elevated expression of manganese superoxide dismutase. *Cancer Res* 54: 4261–4265, 1994.

39. Southern EM. Detection of specific sequences among DNA fragments separated by gel electrophoresis. *J Mol Biol* 98: 503–517, 1975.

40. Spitz DR and Oberley LW. An assay for superoxide dismutase activity in mammalian tissue homogenates. *Anal Biochem* 179: 8–18, 1989.

41. Stadtman ER and Berlett BS. Reactive oxygen-mediated protein oxidation in aging and disease (review). *Drug Metab Rev* 30: 225–243, 1998.

42. Sun Y, Colburn N, and Oberley LW. Depression of catalase gene expression after immortalization and transformation of mouse liver cells. *Carcinogenesis* 14:1505–1510, 1993.

43. Sun Y, Hegamyer G, and Colburn N. Sequence of manganese superoxide dismutase-encoding cDNAs from multiple mouse organs. *Gene* 131: 301–302, 1993.

44. Too, CK, Sierra-Rivera E, Oberley LW, and Guernsey DL. Passage of X-ray-induced immortal, non-transformed phenotype by DNA-mediated transfection. *Cancer Lett*, 97: 39–47, 1995.

45. Towbin H, Staehelin T, and Gordon J. Electrophoretic transfer of proteins for polyacrylamide and gels to nitrocellulose sheets: procedure and some applications. *Proc Natl Acad Sci U S A* 76: 4350–4354, 1979.

46. Williams DE and Reisfeld RA. Disc electrophoresis in polyacrylamide gels: extension to new conditions of pH and buffer. *Ann NY Acad Sci* 121: 373–381, 1964.

47. Woodbury W, Spencer AK, and Stahmann MA. An improved procedure using ferricyanide for detecting catalase isozymes. *Anal Biochem* 44: 301–305, 1971.

48. Yan T, Oberley LW, Zhong W, and St. Clair DK. Manganese-containing superoxide dismutase overexpression causes phenotypic reversion in SV40-transformed human lung fibroblasts. *Cancer Res* 56: 2864–2871, 1996.

49. Zhong W, Oberley LW, Oberley TD, Yan T, Domann FE, and St. Clair DK. Inhibition of cell growth and sensitization to oxidative damage by overexpression of manganese superoxide dismutase in rat glioma cells. *Cell Growth Differ* 7: 1175–1186, 1996.

50. Zhong W, Oberley LW, Oberley TD, and St. Clair DK. Suppression of the malignant phenotype of human glioma cells by overexpression of manganese superoxide dismutase. *Oncogene* 14: 481–490, 1997.

51. Zhong W, Yan T, Lim R, and Oberley LW. Expression of superoxide dismutases, catalase, and glutathione peroxidase in glioma cells. Free *Radic Biol Med* 27: 1334–1345, 1999.

This article has been cited by:

1. Aaron K. Holley, Sanjit Kumar Dhar, Daret K. St. Clair. 2012. Curbing cancer's sweet tooth: Is there a role for MnSOD in regulation of the Warburg effect?. *Mitochondrion* . [CrossRef]

2. Marie Ennen, Vanessa Minig, Stéphanie Grandemange, Nadège Touche, Jean-Louis Merlin, Vanessa Besancenot, Emilie Brunner, Lionel Domenjoud, Philippe Becuwe. 2011. Regulation of the high basal expression of the manganese superoxide dismutase gene in aggressive breast cancer cells. *Free Radical Biology and Medicine* **50**:12, 1771-1779. [CrossRef]

3. Ines Batinic-Haberle, Zrinka Rajic, Artak Tovmasyan, Julio S. Reboucas, Xiaodong Ye, Kam W. Leong, Mark W. Dewhirst, Zeljko Vujaskovic, Ludmil Benov, Ivan Spasojevic. 2011. Diverse functions of cationic Mn(III) N-substituted pyridylporphyrins, recognized as SOD mimics. *Free Radical Biology and Medicine* . [CrossRef]

4. José L. Sardina, Guillermo López-Ruano, Beatriz Sánchez-Sánchez, Marcial Llanillo, Angel Hernández-Hernández. 2011. Reactive oxygen species: Are they important for haematopoiesis?. *Critical Reviews in Oncology/Hematology* . [CrossRef]

5. Anne R. Diers, Brian P. Dranka, Karina C. Ricart, Joo Yeun Oh, Michelle S. Johnson, Fen Zhou, Manuel A. Pallero, Thomas M. Bodenstine, Joanne E. Murphy#Ullrich, Danny R. Welch, Aimee Landar. 2010. Modulation of mammary cancer cell migration by 15-deoxy-# 12,14 -prostaglandin J 2 : implications for anti-metastatic therapy. *Biochemical Journal* **430**:1, 69-78. [CrossRef]

6. Amadou K.S. Camara , Edward J. Lesnefsky , David F. Stowe . 2010. Potential Therapeutic Benefits of Strategies Directed to Mitochondria. *Antioxidants & Redox Signaling* **13**:3, 279-347. [Abstract] [Full Text HTML] [Full Text PDF] [Full Text PDF with Links]

7. Ferdinando Mannello, Gaetana A. Tonti, Andrea Pederzoli, Patrizia Simone, Alessandra Smaniotto, Virginia Medda. 2010. Detection of Superoxide Dismutase-1 in Nipple Aspirate Fluids: A Reactive Oxygen Species–Regulating Enzyme in the Breast Cancer Microenvironment. *Clinical Breast Cancer* **10**:3, 238-245. [CrossRef]

8. Aekyong Kim, Suman Joseph, Aslam Khan, Charles J. Epstein, Raymond Sobel, Ting-Ting Huang. 2010. Enhanced expression of mitochondrial superoxide dismutase leads to prolonged in vivo cell cycle progression and up-regulation of mitochondrial thioredoxin. *Free Radical Biology and Medicine* **48**:11, 1501-1512. [CrossRef]

9. Aaron K. Holley, Sanjit Kumar Dhar, Yong Xu, Daret K. St. Clair. 2010. Manganese superoxide dismutase: beyond life and death. *Amino Acids* . [CrossRef]

10. Regina Brigelius-Flohé, Anna Kipp. 2009. Glutathione peroxidases in different stages of carcinogenesis#. *Biochimica et Biophysica Acta (BBA) - General Subjects* **1790**:11, 1555-1568. [CrossRef]

11. Isabel Quirós, Rosa M. Sáinz, David Hevia, Olivia García-Suárez, Aurora Astudillo, Manuel Rivas, Juan C. Mayo. 2009. Upregulation of manganese superoxide dismutase (SOD2) is a common pathway for neuroendocrine differentiation in prostate cancer cells. *International Journal of Cancer* **125**:7, 1497-1504. [CrossRef]

12. Michael J. Hitchler, Frederick E. Domann. 2009. Metabolic defects provide a spark for the epigenetic switch in cancer. *Free Radical Biology and Medicine* **47**:2, 115-127. [CrossRef]

13. B H Y Yeung, K Y Wong, M C Lin, C K C Wong, T Mashima, T Tsuruo, A S T Wong. 2008. Chemosensitisation by manganese superoxide dismutase inhibition is caspase-9 dependent and involves extracellular signal-regulated kinase 1/2. *British Journal of Cancer* **99**:2, 283-293. [CrossRef]

14. R U Jänicke, D Sohn, K Schulze-Osthoff. 2008. The dark side of a tumor suppressor: anti-apoptotic p53. *Cell Death and Differentiation* **15**:6, 959-976. [CrossRef]

15. Christopher I. van de Wetering, Mitchell C. Coleman, Douglas R. Spitz, Brian J. Smith, C. Michael Knudson. 2008. Manganese superoxide dismutase gene dosage affects chromosomal instability and

tumor onset in a mouse model of T cell lymphoma. *Free Radical Biology and Medicine* **44**:8, 1677-1686. [CrossRef]

16. Zilal Kattan, Vanessa Minig, Pierre Leroy, Michel Dauça, Philippe Becuwe. 2008. Role of manganese superoxide dismutase on growth and invasive properties of human estrogen-independent breast cancer cells. *Breast Cancer Research and Treatment* **108**:2, 203-215. [CrossRef]

17. Christine Hoelzl, Olga Lorenz, Verena Haudek, Nina Gundacker, Siegfried Knasmüller, Christopher Gerner. 2008. Proteome alterations induced in human white blood cells by consumption of Brussels sprouts: Results of a pilot intervention study. *PROTEOMICS – CLINICAL APPLICATIONS* **2**:1, 108-117. [CrossRef]

18. A. Ni#iforovi#, M. Adži#, B. Zari#, M. B. Radoj#i#. 2007. Adjuvant antiproliferative and cytotoxic effect of aloin in irradiated HeLaS3 cells. *Russian Journal of Physical Chemistry A* **81**:9, 1463-1466. [CrossRef]

19. Lisa A. Ridnour , Douglas D. Thomas , Sonia Donzelli , Michael G. Espey , David D. Roberts , David A. Wink , Jeffrey S. Isenberg . 2006. The Biphasic Nature of Nitric Oxide Responses in Tumor Biology. *Antioxidants & Redox Signaling* **8**:7-8, 1329-1337. [Abstract] [Full Text PDF] [Full Text PDF with Links]

20. Dr. Shinya Toyokuni . 2006. Novel Aspects of Oxidative Stress-Associated Carcinogenesis. *Antioxidants & Redox Signaling* **8**:7-8, 1373-1377. [Abstract] [Full Text PDF] [Full Text PDF with Links]

21. Christine J. Weydert, Trent A. Waugh, Justine M. Ritchie, Kanchan S. Iyer, Jenna L. Smith, Ling Li, Douglas R. Spitz, Larry W. Oberley. 2006. Overexpression of manganese or copper–zinc superoxide dismutase inhibits breast cancer growth. *Free Radical Biology and Medicine* **41**:2, 226-237. [CrossRef]

22. C NICCO, A LAURENT, C CHEREAU, B WEILL, F BATTEUX. 2005. Differential modulation of normal and tumor cell proliferation by reactive oxygen species. *Biomedecine & Pharmacotherapy* **59**:4, 169-174. [CrossRef]

23. Terry D. Oberley . 2004. Mitochondria, Manganese Superoxide Dismutase, and Cancer. *Antioxidants & Redox Signaling* **6**:3, 483-487. [Citation] [Full Text PDF] [Full Text PDF with Links]